



Multi-Modal Assessment of Long-Term Erythropoietin Treatment after Neonatal Hypoxic-Ischemic Injury in Rat Brain

Yohan van de Looij^{1,2,*}, Alexandra Chatagner¹, Charles Quairiaux³, Rolf Gruetter^{2,4,5}, Petra S. Hüppi¹, Stéphane V. Sizonenko¹

1 Division of Child Development and Growth, Department of Paediatrics, School of Medicine, University of Geneva and Geneva University Hospital, Geneva, Switzerland, **2** Laboratory for Functional and Metabolic Imaging (LIFMET), Ecole Polytechnique Fédérale de Lausanne (EPFL), Lausanne, Switzerland, **3** Department of Fundamental Neurosciences, School of Medicine, University of Geneva, Geneva, Switzerland, **4** Department of Radiology, University of Lausanne, Lausanne, Switzerland, **5** Department of Radiology, University of Geneva, Geneva, Switzerland

Abstract

Erythropoietin (EPO) has been recognized as a neuroprotective agent. In animal models of neonatal brain injury, exogenous EPO has been shown to reduce lesion size, improve structure and function. Experimental studies have focused on short course treatment after injury. Timing, dose and length of treatment in preterm brain damage remain to be defined. We have evaluated the effects of high dose and long-term EPO treatment in hypoxic-ischemic (HI) injury in 3 days old (P3) rat pups using histopathology, magnetic resonance imaging (MRI) and spectroscopy (MRS) as well as functional assessment with somatosensory-evoked potentials (SEP). After HI, rat pups were assessed by MRI for initial damage and were randomized to receive EPO or vehicle. At the end of treatment period (P25) the size of resulting cortical damage and white matter (WM) microstructure integrity were assessed by MRI and cortical metabolism by MRS. Whisker elicited SEP were recorded to evaluate somatosensory function. Brains were collected for neuropathological assessment. The EPO treated animals did not show significant decrease of the HI induced cortical loss at P25. WM microstructure measured by diffusion tensor imaging was improved and SEP response in the injured cortex was recovered in the EPO treated animals compared to vehicle treated animals. In addition, the metabolic profile was less altered in the EPO group. Long-term treatment with high dose EPO after HI injury in the very immature rat brain induced recovery of WM microstructure and connectivity as well as somatosensory cortical function despite no effects on volume of cortical damage. This indicates that long-term high-dose EPO induces recovery of structural and functional connectivity despite persisting gross anatomical cortical alteration resulting from HI.

Citation: van de Looij Y, Chatagner A, Quairiaux C, Gruetter R, Hüppi PS, et al. (2014) Multi-Modal Assessment of Long-Term Erythropoietin Treatment after Neonatal Hypoxic-Ischemic Injury in Rat Brain. PLoS ONE 9(4): e95643. doi:10.1371/journal.pone.0095643

Editor: Pierre Gressens, Robert Debre Hospital, France

Received: February 18, 2014; **Accepted:** March 27, 2014; **Published:** April 22, 2014

Copyright: © 2014 van de Looij et al. This is an open-access article distributed under the terms of the Creative Commons Attribution License, which permits unrestricted use, distribution, and reproduction in any medium, provided the original author and source are credited.

Funding: This work was funded by the Swiss National Fund (N°31003A-112233 and N°33CM30-124101) and by the ELA Foundation-France (N°ELA 2006-04915). The funders had no role in study design, data collection and analysis, decision to publish, or preparation of the manuscript.

Competing Interests: The authors have declared that no competing interests exist.

* E-mail: yohan.vandelooij@epfl.ch

These authors contributed equally to this work.

Introduction

Neonatal hypoxic-ischemic (HI) brain injuries involve both primary destructive events including neuronal death, gliotic reaction and also secondary maturational disturbances leading to subsequent abnormal development of cerebral white and gray matter [1,2]. These damages lead to altered function that range from severe neurological handicap to behavioral, learning and attention deficits [2]. The postnatal day 3 (P3) rat shares some similarities in terms of cortical neuronal, glial and oligodendroglial development to the very preterm infant (24–28 weeks) [3]. P3-HI injury damages specific brain regions and is characterized by diffuse intracortical white matter loss, zones of patchy neuronal degeneration, altered oligodendrocyte progenitors maturation and subsequent myelination, and hypertrophic astrocytes with formation of gliotic scars [4–7]. These neuropathological features are mainly found in the somatosensory cortex. In direct correlation with the neonatal HI damage of the deep infragranular cortical

area, including the subplate neurons area, P3-HI injured rats show profound functional alteration of neuronal response with a reduced somatosensory amplitude response to whisker stimulus contralateral to the lesioned hemisphere. However, in the first 3 weeks after birth, partial recovery processes take place in the establishment of the sensorimotor cortical networks during the cortical functional maturation period [8].

Erythropoietin (EPO) is a 30.5-kDa cytokine functioning mainly as a survival and differentiation regulator during erythropoiesis [9]. In the central nervous system, neurons, glial cells and cerebral endothelial cells produce EPO and express EPO-receptors (EPO-R) [9]. EPO has been shown to act as an anti-apoptotic, anti-inflammatory and neurotrophic mediator both *in-vitro* and *in-vivo* [9,10]. Several studies documented an autocrine production of EPO not only by astrocytes but also by neurons during conditions of suffering of the cerebral tissue [11,12]. Hypoxic stress increases the production of EPO by the neuronal cells in culture [13]. Further, EPO treatment of neurons in culture reverted glutamate-

induced cell death [14]. In p7 rats, infarct size as a result from neonatal stroke induced by middle cerebral artery occlusion was reduced by EPO administration [15]. In neonatal mice and rats EPO pre-treatment or early after HI insult was also neuroprotective when assessed early at 2–7 days after insult [16–18]. Finally, the neuroprotective effect of EPO treatment after neonatal HI was reported to include a preservation of tyrosine hydroxylase-positive fibers in the ventral tegmental area and substantia nigra pars compacta [19]. EPO has also shown anti-apoptotic effects on oligodendrocytes and promoted neurogenesis and angiogenesis, which are essential for normal neurodevelopment but also injury repair [20,21]. Reducing the initial injury and supporting the subsequent development through neurotrophic factors appear both important mechanisms in neonatal brain injury [22,23].

Magnetic Resonance Imaging (MRI) and Spectroscopy (MRS) are non-invasive MR techniques widely used to assess brain structure and brain metabolism, respectively. Anatomic T₂-Weighted MR images lead to accurate quantification of brain region volumes and has been used to assess lesion volume early after HI as well as long term cortical loss [24]. Diffusion tensor imaging (DTI) is a powerful tool to probe cerebral white matter through a 3D description of water diffusion in the tissue [25]. Changes in diffusivity values (mean: MD, parallel: D_∥ and orthogonal: D_⊥) and/or fractional anisotropy (FA) derived from DTI reveal loss of brain microstructure integrity [26,27]. ¹H magnetic resonance spectroscopy (¹H-MRS) has been used to follow the changes in “neurochemical profile” of the brain during cerebral development [28]. This technique allows assessment of several metabolite concentrations (named as the “neurochemical profile”) known to be altered following HI in the P3 pup rat [24].

Recently, a minimally invasive epicranial approach for multielectrode recordings of vibrissal somatosensory-evoked potentials (SEPs) applied to the P3 neonatal HI model revealed long-term functional deficit [8] and EPO treatment showed sensorimotor recovery after HI injury in the neonatal mice and in spinal cord injury [29,30].

EPO has been shown efficient in different models of term and moderately preterm brain injury [31,32] but has not been used in a very immature P3 HI model. Further, only short-term protective treatment regimens have been evaluated. In the present study, we investigated the neuroprotective effects, including damage reduction and neurotrophic action, of long-term high dose EPO administration in the P3-HI model using a multi-modal strategy that combine histological, macro-structural (MRI), micro-structural (DTI), neurochemical (MRS) as well as functional (SEP) assessments.

Materials and Methods

All animal experiments were approved by the Swiss Veterinary Office and in adequacy with Swiss animal welfare laws. The unilateral P3 moderate HI model has been described previously [6,7]. Briefly, P3 male Wistar pups underwent right carotid artery cauterization under isoflurane anesthesia then after 30 minutes recovery rat pups were exposed to 6% O₂ hypoxia for 30 minutes under thermoneutral conditions.

Magnetic Resonance Imaging: T₂-Weighted Images

All *in-vivo* MR experiments were performed on an actively-shielded 9.4T/31 cm magnet (Magnex Scientific, Abington, UK; Varian, Palo Alto, CA, USA) equipped with 12-cm gradient coils

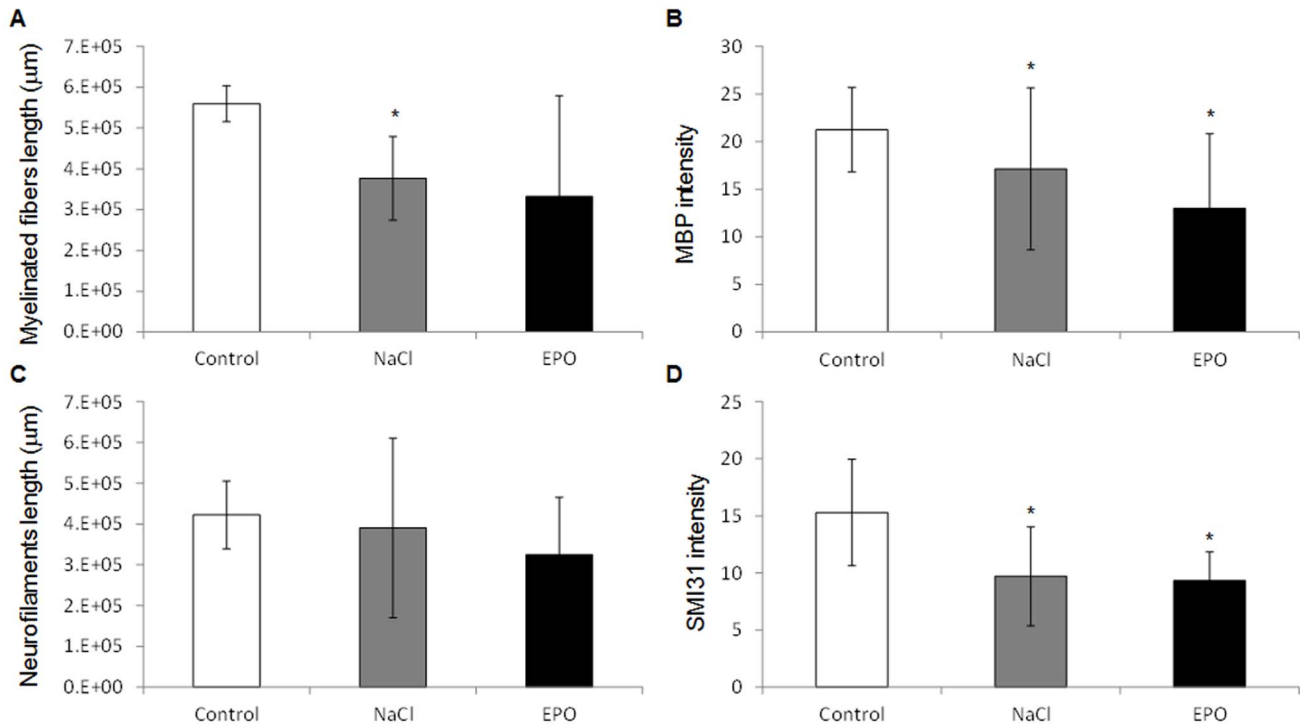


Figure 1. Myelination and neurofilaments in the ipsilateral cortex. A) Total length of myelinated fibers (μm) of MBP positive stained fibers in the cortex of Control, NaCl and EPO treated rats. B) MBP average fluorescence intensity in the cortex of Control, NaCl and EPO treated rats. C) Total length of neurofilaments (μm) of SMI31 stained fibers in the cortex of Control, NaCl and EPO treated rats. D) SMI31 average fluorescence intensity in the cortex of Control, NaCl and EPO treated rats. All the data are presented as mean ± SD, *: $P < 0.05$, NaCl vs. Control and EPO vs. Control, $n = 12$ rats for each group, NaCl, EPO and Control.
doi:10.1371/journal.pone.0095643.g001

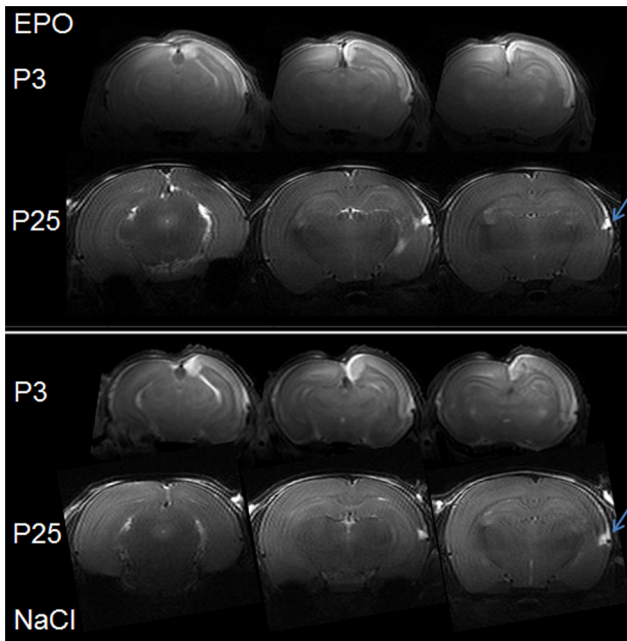


Figure 2. T₂ weighted MRI at P3 and P25. T₂ weighted images of typical EPO and NaCl treated pup rats at 5 h (P3) and 22 d (P25) after injury showing the evolution of the ischemic lesion in the ipsilateral cortex (right). At P3, ischemic lesion appears as hypersignal. At P25, images present a large cortical loss in the ipsilateral cortex and an abnormal development for the both groups. Remaining trace of lesion was observed for the both groups at the bottom of the cortex (arrows). doi:10.1371/journal.pone.0095643.g002

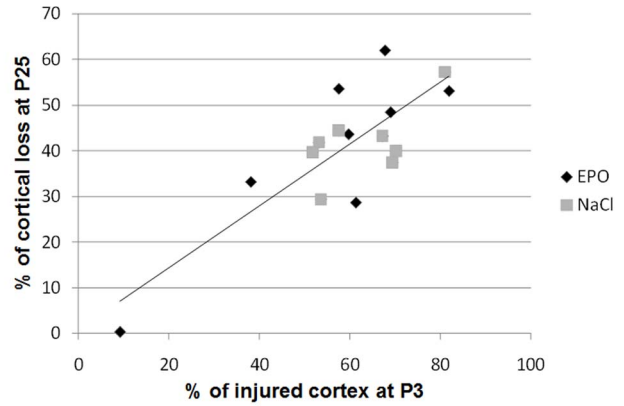
(400 mT/m, 120 μs) with a quadrature transceive 17-mm surface RF coil. During measurements, each pup was placed supine within an adapted holder and continuously anesthetized under a flow of 1.5–2% isoflurane in oxygen. Body temperature was maintained at 37°C using thermoregulated water circulation. 5 h following HI, T₂W Fast Spin Echo (FSE) images with TE/TR = 80/6000 ms; FOV = 25×25 mm and matrix size = 256×128 were used to detect presence of injury as well as determinate the initial lesion volume. Only the pups showing hyper-intense signal in the ipsilateral hemisphere on these acute T₂W images were randomized for the therapeutic intervention.

EPO Treatment

Animals showing injury on initial MRI were selected and randomized to NaCl group, injected intraperitoneally with NaCl 0.9% or to EPO group, injected intraperitoneally with recombinant human EPO (rhEPO, Roche, Basel, Switzerland) 10 U/g body weight/day during the first week after HI (P3 to P10) and then 5 U/g body weight 3×/week until P25. A Control group, which was not subjected to surgery and injection, was also studied.

¹H Magnetic Resonance Spectroscopy

To study the effects of the treatment on brain metabolic profile, 22 days following HI (P25), ¹H-MRS was performed. At P25, FSE images using the same parameters as at P3 were performed for positioning of ¹H-MRS voxel of interest (1.5×1.5×2.5 mm³). Spectra acquisition was performed as previously described [24] using an ultra-short echo time (TE/TR = 2.7/4000 ms) SPECIAL spectroscopy method [33]. Measurements were made in the area of somatosensory cortex as reported previously [5–7,24] as well as the corresponding cortical area for the Control group (n = 8 rats



% Inj. Cx P3		% Cort. loss P25	
EPO	NaCl	EPO	NaCl
38.8±16.4	41.4±9.9	40.4±19.5	41.7±7.8

Figure 3. Volumes of cortical injury at P3 and loss at P25. Upper panel: percentage of cortical loss at P25 as a function of the percentage of injured cortex at P3 for the both groups: EPO and NaCl. A strong correlation independent of the group was found: R² = 0.67; P = 0.0001. Lower panel: percentage of injured cortex (Inj. Cx) at P3 and percentage of cortical loss (% Cort. loss) at P25 for EPO and NaCl groups. There were no statistical differences between EPO and NaCl groups in terms of cortical injury at P3 and loss at P25. Data are presented as mean ± SD, n = 8 rats for each group, NaCl, EPO and Control. doi:10.1371/journal.pone.0095643.g003

for each group, NaCl, EPO and Control). 70 series of FIDs (12 averages each) were acquired, individually corrected for frequency drift, summed together and corrected for residual eddy current effects using the reference water signal. Proton spectra were analyzed with LCModel [34] as previously described [24]. Metabolites were quantified resulting in a neurochemical profile of the cortical lesion for the EPO and NaCl groups and of the cortex in the Control group.

Volumetric Measurements

From FSE images, volumetric measurements were performed using Anatomist/Brain Visa [35]. At P3, lesion volume (LV) as well as ipsilateral cortical volume (ICV) was measured; at P25 contralateral cortical volume (CCV) as well as ipsilateral cortical volume (ICV) was quantified. Volumetric measurements resulted in percentage of injured cortex (= (LV/ICV)×100) at P3 and percentage of cortical loss (= [(CCV-ICV)/CCV]×100) at P25 (n = 8 rats for each group, NaCl and EPO).

Somatosensory-evoked Potentials (SEPs) Recordings

Following ¹H-MRS, epicranial recordings of somatosensory evoked potentials (SEP) were carried out at P27–P28 under isoflurane anesthesia as previously described [8] (n = 11, 10 and 9 rats for NaCl, EPO and Control group, respectively). Before surgery, anesthesia was induced with 3–4% isoflurane then rats were mounted in a stereotaxic frame. Isoflurane was lowered at 2.5% and local bupivacaine anesthesia was applied to the scalp. The skull was exposed by retracting the skin from the frontal to the occipital bones. A 16 steel electrodes grid dipped in EEG paste (500 μm in diameter, final impedance ≈ 50 kOhms) was applied on the skull, covering the entire exposed surface (see [8] for electrode coordinates). SEP were recorded at 0.7–1% isoflurane with a custom-made amplifier (gain 5000X; band pass filters 1–

500 Hz, analog to digital conversion at 2 KHz [8]). During recordings, absence of withdrawal hind limb reflex was controlled and body temperature was maintained at 37°C using a heating pad.

Unilateral somatosensory stimuli were delivered simultaneously to all large whiskers on one side of the snout through a solenoid-based stimulator device [8,36]. Stimuli consisted of 500 μm back-and-forth deflections with 1 ms rise time. Right-sided and left-sided series of 50 stimuli were applied with an inter-stimulus interval of 9 seconds.

Individual SEPs were calculated offline by averaging responses 100 ms prestimulus to 500 ms poststimulus. Maximum positive voltage peaks were measured for each SEP at right and left S1 electrodes (e4, e12).

Ex-vivo Diffusion Tensor Imaging

Following SEPs, animals received an overdose of intraperitoneal injection of sodium pentobarbital and were transcardially perfused with NaCl 0.9% followed by with 4% paraformaldehyde on 0.1% PBS for tissue fixation. DTI experiments on *ex-vivo* brain were performed with a transceiver 25-mm birdcage RF coil ($n = 6$ rats for each group, NaCl, EPO and Control). Spin Echo sequence ($TE/TR = 30/5000$ ms) was used, diffusion gradients were applied along dual gradient diffusion gradient sampling scheme [25] ($G_{\text{diff}} = 22$ G/cm, $\delta = 3$ ms and $\Delta = 20$ ms given a b -value of 1184 s. mm^{-2}). 20 slices of 0.8 mm thickness with an in-plane pixel size of 70 μm were acquired in the axial plane. Using a homemade Matlab (Mathworks, Natick, MA, USA) software [27,37], region of interest (ROI) were manually delineated on four different regions of the brain: the external capsule (EC), the internal capsule (IC), the corpus callosum (CC) and the superficial layer of sensorimotor cortex (Cx) at four different levels of the brain corresponding to the genu, the body (2 different parts of the body) and the splenium of the corpus callosum.

Immunohistology

Ex-vivo imaged brains added with non-scanned ones at P25 were used for immunohistological studies ($n = 8$ rats for each group, NaCl, EPO and Control). Anti-Glial fibrillary acid protein (anti-GFAP, Dako, ZO334, Glstrup, Denmark) and anti-Neuronal Nuclei (anti-NeuN, Chemicon, Billerica, MA, USA) staining were used to observe the long-term effects of EPO on astrocytes activation, resulting in formation of gliotic scar and on neuronal death and survival, respectively. Anti-Myelin basic protein antibody (anti-MBP, Chemicon, Billerica, MA, USA) was used to determine white matter injury with altered myelination. Anti-Neurofilament antibody (anti-SMI 31, Chemicon, Billerica, MA, USA) was used to assess neurofilament integrity.

After brain fixation as previously described, pup brains were cryoprotected in 30% sucrose and frozen. Contiguous 12 μm sections at the level of the dorsal hippocampus were cut on a cryostat and collected on superfrost slides (ThermoScientific, Waltham, MA, USA). Immunostaining was performed using the following protocol: sections were washed in a 0.1% PBS and non-specific binding was blocked by incubating the slides in 0.1% PBS/5% BSA/0.3% triton/3% normal goat serum (NGS). They were then incubated overnight at 4°C with the different primary antibodies: NeuN 1:200 in 0.1 M PBS/pH 7.4/5% BSA/1% NGS, GFAP 1:400 in 0.1 M PBS/pH 7.4/5% BSA/1% NGS, MBP 1:200 in 0.1 M PBS/pH 7.4/5% BSA/1% NGS and SMI 31 1:200 in 0.1 M PBS/pH 7.4/5% BSA/1% NGS. This was followed by 2 hours incubation at room temperature with secondary goat Alexa 488 anti-rabbit 1/1000 (Lifetechnologies, Carlsbad, CA, USA) for GFAP and Goat Alexa 555 anti-Mouse

1/1000 (Lifetechnologies, Carlsbad, CA, USA) for NeuN, MBP and SMI 31 in 0.1 M PBS/pH 7.4/5% BSA/1% NGS. Slides were finally washed and cover slipped with mounting media.

For each specific staining and each brain, three slides of 220 μm sections apart were scanned using the Mirax (Zeiss, Göttingen, Germany) and analyzed. GFAP-positive staining was evaluated in the ipsilateral cortex of HI animals. A scoring system with scores ranging from 0 (no gliotic scar) to 4 (strong staining covering the whole surface of parietal cortex in the deeper layers) was used.

Other immunostaining were evaluated in Metamorph (Molecular Devices, Sunnyvale, CA, USA) using specific automated journals defined for desired unbiased quantification. The quantification of neurons was done by counting DAPI and NeuN positive cells in both cortices of each animal for the three groups leading to number of neurons in the ipsilateral and contralateral cortices for each group (NnI and NnC, respectively). The percentage of neuronal loss in the ipsilateral cortex was then calculated using the formula: $((\text{NnC}-\text{NnI})/(\text{NnC}+\text{NnI})) \times 100$, for each group.

The same automated journal was used to quantify length of myelinated fibers (from MBP staining) and neurite outgrowth (from SMI 31 staining). Briefly, first the skeletons of the fibers were detected and measured and, second the distance from the cortex surface to the extremity of the fibers was measured. Finally, the second distance was subtracted to the first one, resulting in a fiber length taking into account the cortical thickness. Resulted lengths were all summed together leading to total length of myelinated fibers and total length of neurofilaments in the ipsilateral cortex for each rat of the three groups.

The average fluorescence intensity for MBP and SMI 31 positive staining deducted from the background was assessed in the entire surface of ipsilateral cortices within each animal of the three groups. In the genu of the corpus callosum, in the internal and external capsule, three ROI having the same surface were drawn in each zone and immunofluorescence was measured. The background was subtracted and the mean of the three zones was calculated, indicating the level of myelination and of intact neurofilaments in these areas.

Statistical Analysis

All the data are presented as mean \pm standard deviation (SD) except for SEP results presented as mean \pm standard error of the mean (SEM). For MRI-MRS and immunohistology, a Wilcoxon test was used to compare values between ipsilateral and contralateral sides of the same animal and a Mann-Whitney test to compare statistically values between the groups ($n = 8$ for each group), both using Matlab (Mathworks, Natick, MA, USA). For SEPs, as voltage peaks and ratio distributions turned out to be normal, ANOVA and t-tests were applied for between and within group comparisons. Analyses were performed using Cartool (<http://brainmapping.unige.ch/Cartool.htm>) and Matlab (Mathworks, Natick, MA, USA).

Results

At the end of the treatment period, hemoglobin and hematocite were measured in both NaCl and EPO treated animals and no difference was seen.

Astroglial Scar Formation

GFAP-positive staining was present in the ipsilateral cortex of HI animals. Various degrees of astrogliosis in layers IV, V, VI in the parietal cortex of the right injured hemisphere were observed. In the NaCl group, 28.55% of animals showed a score of 0, 14.25% a score of 1, 28.55% a score of 2 and 28.55% a score of 3.

In the EPO group, 42.85% showed a score of 0, 14.25% a score of 1, 28.55% a score of 3 and 14.25% a score of 4. No significant score difference was found between NaCl and EPO groups.

Neuronal Loss Assessment

Quantification of neurons revealed a significant increase of neuronal loss in NaCl compared to Control groups ($19.1 \pm 13.9\%$ vs. $0.9 \pm 1.4\%$, respectively; $P \leq 0.0001$) as well as between EPO and Control groups ($30.9\% \pm 25.1$ vs. $0.9\% \pm 1.4$ $P \leq 0.0001$). No significant difference was observed between EPO and NaCl groups.

Myelin Staining

In the cortex, myelination along the fibers measured as the total cortical MBP positive fibers (figure 1A) was reduced in NaCl compared to Control groups ($376768 \mu\text{m} \pm 102627$ and $559701 \mu\text{m} \pm 43771$, respectively; $P = 0.007$) while there was no significant difference neither between EPO and Control groups ($331953 \pm 247332 \mu\text{m}$ and $559701 \pm 43771 \mu\text{m}$, respectively) nor between NaCl and EPO groups.

The average fluorescent intensity of MBP staining (figure 1B) was significantly reduced in the EPO compared to Control (12.98 ± 7.85 and 21.25 ± 4.43 , respectively; $P = 0.014$) as well as in the NaCl compared to Control groups (17.13 ± 8.5 and 21.25 ± 4.43 , respectively; $P = 0.011$). EPO group vs. NaCl group presented no significant difference. In the corpus callosum, in the external and internal capsules, the quantifications of the MBP fluorescent signal did not reveal any significant difference between the groups Control, NaCl and EPO (data not shown).

Neurofilaments

In the cortex, the analysis of neurofilaments length (figure 1C) did not reveal any significant difference between NaCl, EPO and Control groups ($324970 \pm 140475 \mu\text{m}$, $390235 \pm 220066 \mu\text{m}$ and $422241 \pm 82999 \mu\text{m}$, respectively). In the other hand, the average fluorescent intensity of SMI 31 staining (figure 1D) was significantly reduced in the EPO compared to Control groups (9.32 ± 2.51 vs. 15.29 ± 4.66 , respectively; $P = 0.04$) as well as between the NaCl and Control groups (9.69 ± 6.38 vs. 15.29 ± 4.66 , respectively; $P = 0.02$). There was no significant difference between NaCl and EPO groups. No significant difference was observed in the corpus callosum, external and internal capsules, in SMI 31 quantifications between the three groups (data not shown).

Cortical Volumes

Figure 2 shows multi-slice T_2 -weighted FSE brain images of a typical EPO and NaCl treated pup rat at different time points (5 h (P3) and 22 d (P25) after injury) showing the evolution of the ischemic lesion in the ipsilateral cortex for the both groups. At P3, ischemic lesion appears in hypersignal due to the presence of edema (figure 2). At P25 for the both groups, a small residual T_2 hypersignal was observed (figure 2, arrows) at the level of the rhinal fissure. No cyst was present but images showed cortical loss in the ipsilateral hemisphere in both groups. There was no difference in the percentage of injured cortex at P3 before treatment randomization between EPO and NaCl groups ($38.8 \pm 16.4\%$ vs. $41.4 \pm 9.9\%$ for EPO and NaCl, respectively) showing the homogeneity of injury in both groups. A strong correlation independent of the groups was found between the percentage of injured cortex at P3 and the percentage of cortical loss at P25 (figure 3, $R^2 = 0.67$; $P = 0.0001$). At P25, the percentage of cortical loss was not different between EPO and

NaCl treated pups ($40.4 \pm 19.5\%$ vs. $41.7 \pm 7.8\%$ for EPO and NaCl, respectively).

Metabolic Profile of Cortex

Good spectral quality was achieved in the current study, as judged from water linewidth, obtained with FASTMAP, ranging from 8 Hz to 12 Hz. Due to very thin cortical structure in the rat pup brain, MRS was performed on a very small volume of $12 \mu\text{l}$ placed on the cortex (figure 4). On the overall study signal to noise ratio was equal in average to 15 ± 3 . These consistent data were subjected to spectral analysis and absolute quantification using an LCModel. It should be noticed that the voxel of interest was always placed higher than the remaining T_2 hypersignal previously described, avoiding a possible water contamination in the metabolite quantifications.

Table 1 summarizes the changes observed on metabolite concentrations. Comparing ipsilateral and control cortices, for both the NaCl group and the EPO group significant decrease of [Glu] as well as [totalNAA], [Glu]+[Gln] and [totalCr] was observed in the lesion area. In addition in NaCl group, [NAA], [Cr] and [PCr] were also significantly decreased in the injured cortex. Ipsilateral cortical “neurochemical profiles” of EPO versus NaCl did not show any significant difference.

Somatosensory Evoked Potentials

To analyze the effect of the EPO treatment on functional recovery, we recorded SEP in response to whisker stimulation (figure 5A). As already described in previous studies [8], the earliest and strongest SEP component in response to unilateral whisker stimulation shows the activation of the contralateral S1 region in control and in HI groups (figure 5B). The topographic voltage maps at the peak amplitude of this SEP component suggest a deficit in the amplitude of the response to left-sided whisker stimuli in the right S1 cortices of the NaCl as compared to the control and EPO groups as well as to the response to right-sided whisker stimuli in their left, non-injured, hemisphere. No significant difference was found in the mean voltage peak amplitudes recorded above S1 in the non-injured hemisphere between the 3 groups (Mean \pm SEM: control: $461 \pm 84 \mu\text{V}$; NaCl = $507 \pm 94 \mu\text{V}$; EPO = $388 \pm 83 \mu\text{V}$; $P = 0.65$, one-way AN-

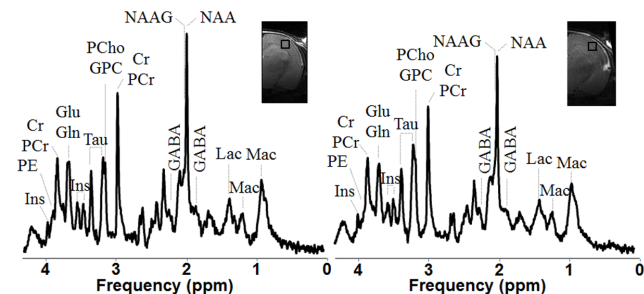


Figure 4. Metabolic profile of cortex. Typical in vivo localized ^1H -NMR spectra at 9.4T in the ipsilateral cortex of one NaCl treated rat pup (right) as well as in the same area of a Control rat cortex with respective metabolite assignments. All spectra (SPECIAL, TE/TR = 2.8/4000 ms, NT = 840) were displayed with Gaussian apodization ($gf = 0.11$ s) and scaled relative to the concentration of macromolecules. Abbreviations: Mac, macromolecules; Asc, ascorbate; Asp, aspartate; GPC, Glycerophosphocholine; PCho, phosphorylcholine; Cr, creatine; PCr, phosphocreatine; GABA, γ -aminobutyric acid; Glc, glucose; Glu, glutamate; Gln, glutamine; Ins, myo-inositol; Lac, lactate; NAA, N-acetylaspartate; NAAG, N-acetylaspartylglutamate; PE, phosphoethanolamine and Tau, taurine. doi:10.1371/journal.pone.0095643.g004

Table 1. Neurochemical profiles.

	EPO	vs. CTL	NaCl	vs. CTL	CTL
Mac	1.8±0.1		1.8±0.1		1.9±0.2
Cr	3.1±0.5		3.0±0.5	* ↓	3.6±0.5
PCr	4.5±2.2		3.5±0.6	** ↓	4.2±0.5
Glc	4.2±3.2		2.9±0.8		3.7±3.1
Gln	2.6±0.6		2.9±0.4	* ↓	3.3±1.0
Glu	7.1±0.9	** ↓	6.9±1.6	* ↓	9.3±1.3
NAA	7.6±1.4		7.2±0.9	** ↓	9.0±0.8
Tau	6.5±1.2		6.2±1.7		7.5±0.6
NAA+NAAG	8.3±1.3	* ↓	8.0±0.9	** ↓	9.9±1.0
Glu+Gln	9.6±1.0	*** ↓	9.8±1.8	* ↓	12.6±1.8
GPC+PCho	0.5±0.2		0.6±0.2		0.6±0.2
Cr+PCr	7.3±1.7	* ↓	6.5±0.9	** ↓	7.9±0.8
PCr/Cr	1.1±0.2		1.2±0.3		1.2±0.2
Glu/Gln	2.9±0.9		2.4±0.5		3.0±0.9

Metabolite concentrations in the ipsilateral cortex of EPO and NaCl treated rat pups as well as in the control cortex, and summary of observed metabolite changes following HI in the EPO and NaCl treated rats when compared to the control rats. Changes are displayed with specific orientated arrows: "↑", increase and "↓", decrease. The number of "*" represents significant level of $P < 0.05$, 0.01, 0.001 respectively. Notice that no significant difference was found between EPO and NaCl cortices. All concentrations are presented as mean \pm SD in mM/g except the ratios. Abbreviations: Mac, macromolecules; Asc, ascorbate; Asp, aspartate; GPC, Glycero-phosphocholine; PCho, phosphorylcholine; Cr, creatine; PCr, phosphocreatine; GABA, γ -aminobutyric acid; Glc, glucose; Glu, glutamate; Gln, glutamine; Ins, myo-inositol; Lac, lactate; NAA, N-acetylaspartate; NAAG, N-acetylaspartylglutamate; PE, phosphoethanolamine and Tau, taurine.
doi:10.1371/journal.pone.0095643.t001

OVA; figure 5C). However the SEP peak amplitude is greatly reduced in the right injured hemisphere of the NaCl group compared to the control group with the EPO group showing an intermediate SEP peak amplitude reduction (Mean \pm SEM: control: 463 ± 73 μ V; NaCl = 291 ± 58 μ V; EPO = 359 ± 53 μ V). ANOVA analyses failed to show a group effect because of the variability of the SEP voltage values between individuals. However, within group comparisons using paired statistics revealed in the animals of the NaCl group a strong and significant reduction of contralateral SEP amplitude in the right hemisphere as compared to contralateral SEP in their left hemisphere ($P = 0.02$, paired t-test, two tailed). No difference was found between contralateral SEPs both in the control and in the EPO groups. Accordingly, the mean SEP ratios between right and left peak amplitudes was significantly different between groups ($P = 0.04$; ANOVA): while the right/left ratio is around 100% in the control and the EPO groups, a strong bias is observed in the NaCl group, with a mean value in the injured hemisphere reaching only $62 \pm 9\%$ of the contralateral side (Figure 5D). Such a bias indicates reduced amplitude of the response in the injured hemisphere however a mechanism of compensation in the contralateral non-injured hemisphere may also participate to the bias of the SEP in the NaCl group following the unilateral lesion.

Microstructure Evaluation by DTI

Direction encoded brain color maps of a typical EPO and NaCl treated pup rats are presented on figure 6. The excellent SNR and resolution (70 μ m in-plane) of these images allowed an accurate estimation of diffusion tensor derived parameters. No obvious visual differences appeared between the two maps. Abnormal development was obvious for both rats with a dissymmetry between ipsilateral and contralateral hemispheres (*i.e.* thinner cortex in the injured hemisphere due to cortical loss following injury). The contralateral hemisphere was comparable to the one of the control group (not shown). It should be noticed that these

diffusion data were acquired on *ex-vivo* fixed brain, thus the diffusivity values are significantly lower than *in-vivo* acquisition whereas FA values remained unchanged after fixation as previously described [38].

FA measurements were made at four different levels of the brain on axial slice corresponding to the levels of the genu, the body (2 image-planes) and the splenium of the corpus callosum. ROIs are overlaid on direction encoded color maps on figure 6. Results are presented as mean values over the four different levels (Figure 7). In the IC, EC and CC, FA values were found significantly lower in the NaCl group compared with Control group whereas there was no significant difference between EPO and controls. Only in the CC, a significant difference in FA values was observed between EPO and NaCl. In the EC, FA = 0.51 ± 0.02 , 0.44 ± 0.05 , 0.49 ± 0.03 for Control, NaCl and EPO, respectively; in the IC, FA = 0.49 ± 0.04 , 0.41 ± 0.05 , 0.45 ± 0.04 for Control, NaCl and EPO, respectively and in the CC, FA = 0.65 ± 0.04 , 0.49 ± 0.05 , 0.59 ± 0.04 for Control, NaCl and EPO, respectively. This FA decrease was related to a significant increase of the radial diffusivity. In the EC, $D_{\perp} = 2.07 \pm 0.17 \times 10^{-4} \text{ mm}^2 \cdot \text{s}^{-1}$, $2.54 \pm 0.17 \times 10^{-4} \text{ mm}^2 \cdot \text{s}^{-1}$, $2.42 \pm 0.46 \times 10^{-4} \text{ mm}^2 \cdot \text{s}^{-1}$ for Control, NaCl and EPO, respectively; in the IC, $D_{\perp} = 2.21 \pm 0.19 \times 10^{-4} \text{ mm}^2 \cdot \text{s}^{-1}$, $2.58 \pm 0.27 \times 10^{-4} \text{ mm}^2 \cdot \text{s}^{-1}$, $2.47 \pm 0.42 \times 10^{-4} \text{ mm}^2 \cdot \text{s}^{-1}$ for Control, NaCl and EPO, respectively and in the CC, $D_{\perp} = 1.58 \pm 0.17 \times 10^{-4} \text{ mm}^2 \cdot \text{s}^{-1}$, $2.41 \pm 0.26 \times 10^{-4} \text{ mm}^2 \cdot \text{s}^{-1}$, $2.26 \pm 0.50 \times 10^{-4} \text{ mm}^2 \cdot \text{s}^{-1}$ for Control, NaCl and EPO, respectively. In the cortex, no significant difference was found between the groups (NaCl, EPO and Control) neither on diffusivity values, nor on FA (Figure 7).

Discussion

Using different approaches we aimed at evaluating the protective role of long-term high dose of EPO treatment after moderate HI injury in the immature P3 rat brain. In this study,

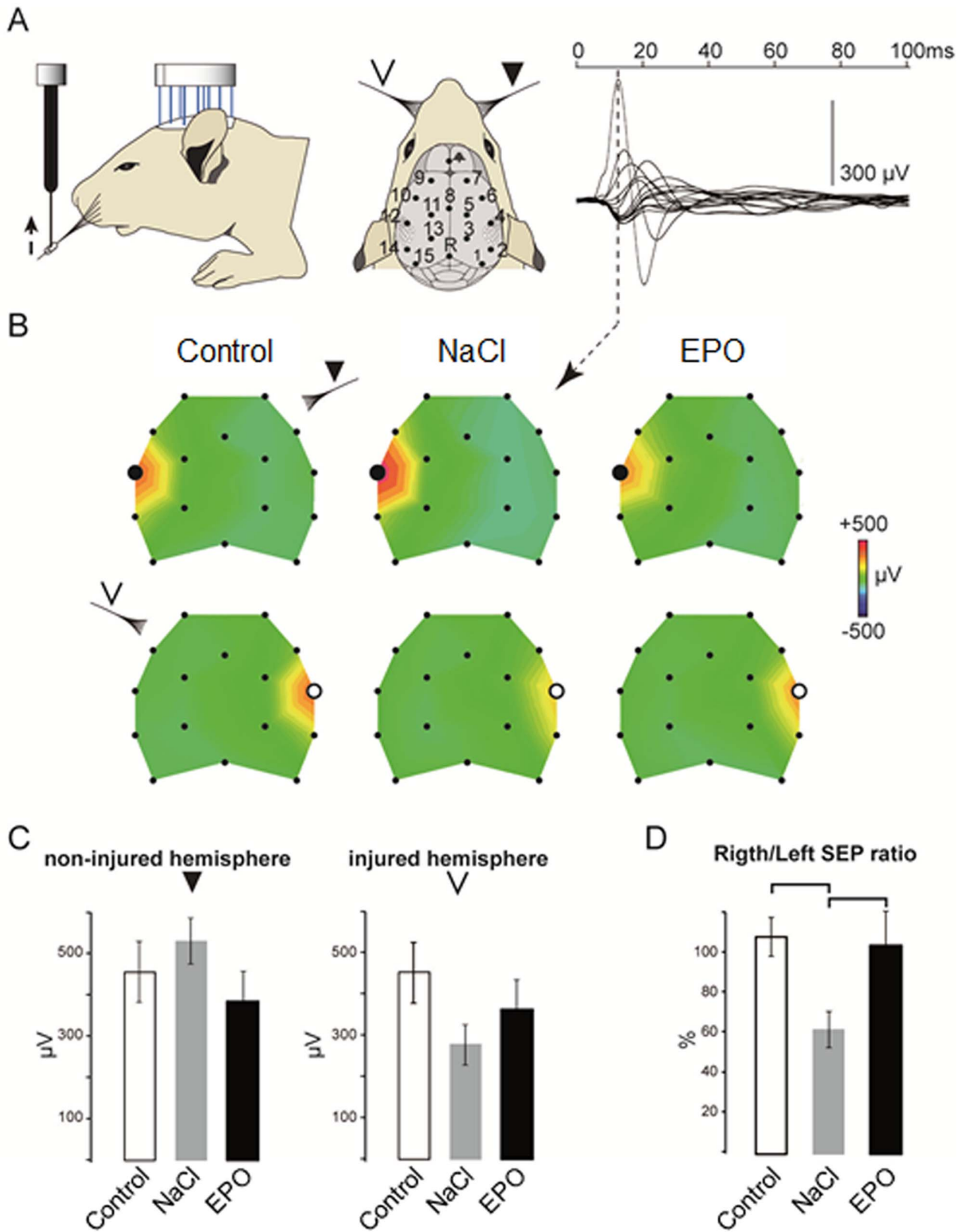


Figure 5. Functional evaluation with SEP. A. Design of the epicranial recording setup. SEPs were recorded in response to unilateral left-sided or right-sided whisker stimuli using an array of 16 epicranial electrodes (n = 11, 10 and 9 rats for NaCl, EPO and Control group, respectively). On the right, an example of the average superimposed SEP traces of all electrodes recorded in one control animal in response to 50 right whisker stimuli. The dashed line indicates the time of the peak positive response typically recorded at the contralateral S1 electrode and characterizing the first SEP component. B. Color-coded voltage maps at the time of the peak response of the grand average for right-sided (upper row) and left-sided (lower row) stimuli. C. Average SEP amplitude (μV) in the non-injured hemisphere (left) and injured hemisphere (right) for Control, NaCl, and EPO groups. D. Right/Left SEP ratio for Control, NaCl, and EPO groups.

stimulation in the Control, NaCl and EPO groups. C. Histograms showing for all groups the mean \pm SEM voltage amplitude for the peak SEP response at the S1 electrode (white dots) in the non-injured (right, e12) and injured (left, e4) hemispheres in response to contralateral stimuli. D. Mean \pm SEM ratios calculated between peak SEP amplitudes at the S1 electrodes.
doi:10.1371/journal.pone.0095643.g005

long-term EPO treatment HI injury in the P3 rat brain did not provide gross cortical grey matter protection but showed partial protective effects on metabolism, white matter structure and somatosensory function. The neurochemical profile of EPO treated rats presented less significant changes than the one of NaCl treated rats. EPO protected the integrity of several white matter tracts as depicted by normalized DTI derived parameters values at P25. From a functional point of view, long-term EPO treatment after P3 HI brain injury promoted whisker stimulated somatosensory functional recovery at P27–P28 to near normal levels.

In a previous study we observed that females rat pups showed smaller injury after HI injury at P3 with better recovery and reduced cortical damage at P25 compared to males [24]. As a consequence of this differential level of damage and recovery, evaluation of EPO effects on HI injury in P3 females would have been difficult to distinguish from the spontaneous recovery in absence of treatment. For this reason, in this therapeutic study we chose to treat and assess male pups only.

There is an important number of published studies of EPO given prior or after a neonatal insult in mice or rats that showed a reduction of the damage with decrease of cell death, not only neurons but also oligodendrocytes with preserved myelination [31,32]. Furthermore, when administrated acutely after neonatal ischemia, EPO is not only neuroprotective but also stimulates angiogenesis and neurogenesis [39]. It is important to notice that in the majority of these studies, assessment of brain damage was performed a few days after the insult and after short-term

treatment only. Moreover, most of these neonatal models of injury did use older pups with a more mature brain at time of injury and treatment. Further, these models are more severe with mild to severe brain damage compared to the one used in this study. Our study investigated a long-term treatment of EPO during 3 weeks with high dose (10 U/g) of EPO during the first week. This treatment regimen does not show similar neuroprotection compared to the shorter therapeutic intervention but it is also difficult to compare as in these studies EPO effect was assessed earlier. A previous study reported that an early administration of EPO over a period of 1 week after HI on P7 rats resulted in reduced infarct volume, significant enhancement of functional revascularization and neuronal replacement in the ischemic hemisphere [15]. In our study, despite early and sustained EPO administration no reduction of infarct size at P25 was seen with any increased neuronal survival measured by NAA concentration and neuronal counts in the EPO group. Moreover, exogenous EPO did not attenuate astrogliosis as depicted by the 50% of EPO treated animals showing significant glial scarring not different from the untreated animals. In the ipsilateral cortices of EPO treated rats, astrogliosis was present and very strong or completely absent. This might be dependent on the extent of the primary injury at P3 as a variability of the lesion size is observed at this time point as depicted by the standard deviation of the percentage of injured cortex at P3. Indeed the degree or nature of the injury itself in the acute phase may elicit differential level of therapeutic effect of EPO. One potential mechanism for these differential actions of EPO under different degrees of injury may be the regulation of

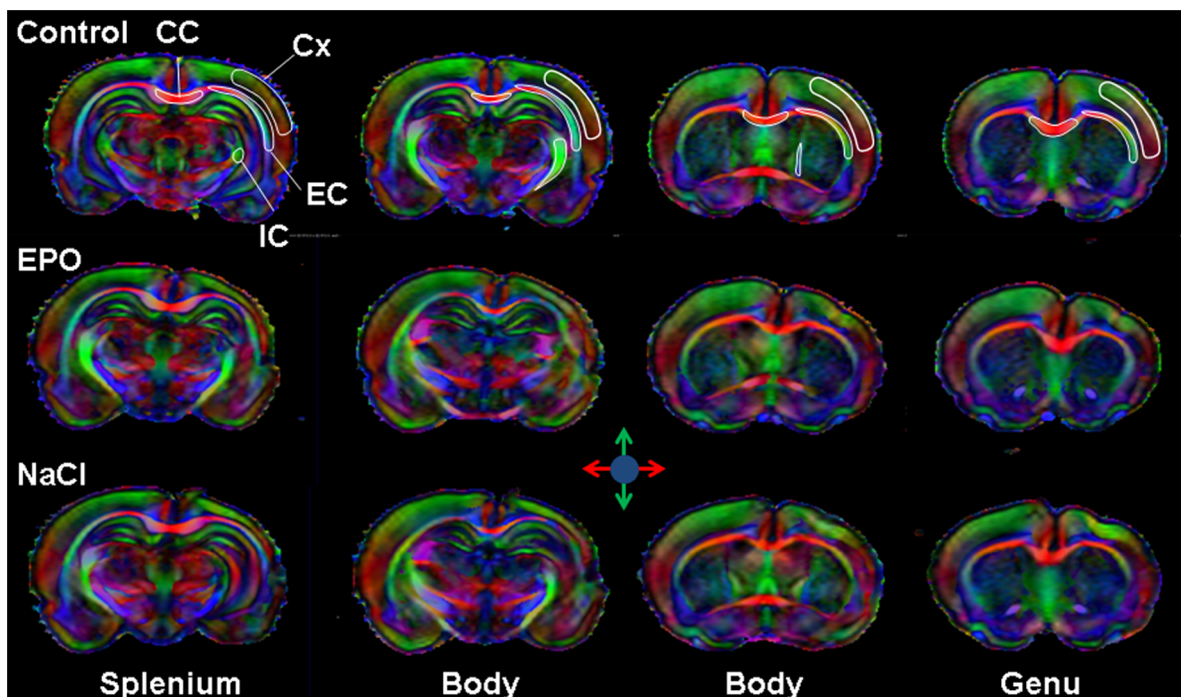


Figure 6. DTI analysis of microstructure. Direction encoded color maps of typical P25 Control, EPO and NaCl pup rat brain at four different image-planes corresponding to the four levels of DTI indices measurements: Splenium, Body, Body and Genu of the corpus callosum. The different ROIs analyzed are overlaid on the Control map: external capsule (EC), internal capsule (IC), corpus callosum (CC) and cortex (Cx).
doi:10.1371/journal.pone.0095643.g006

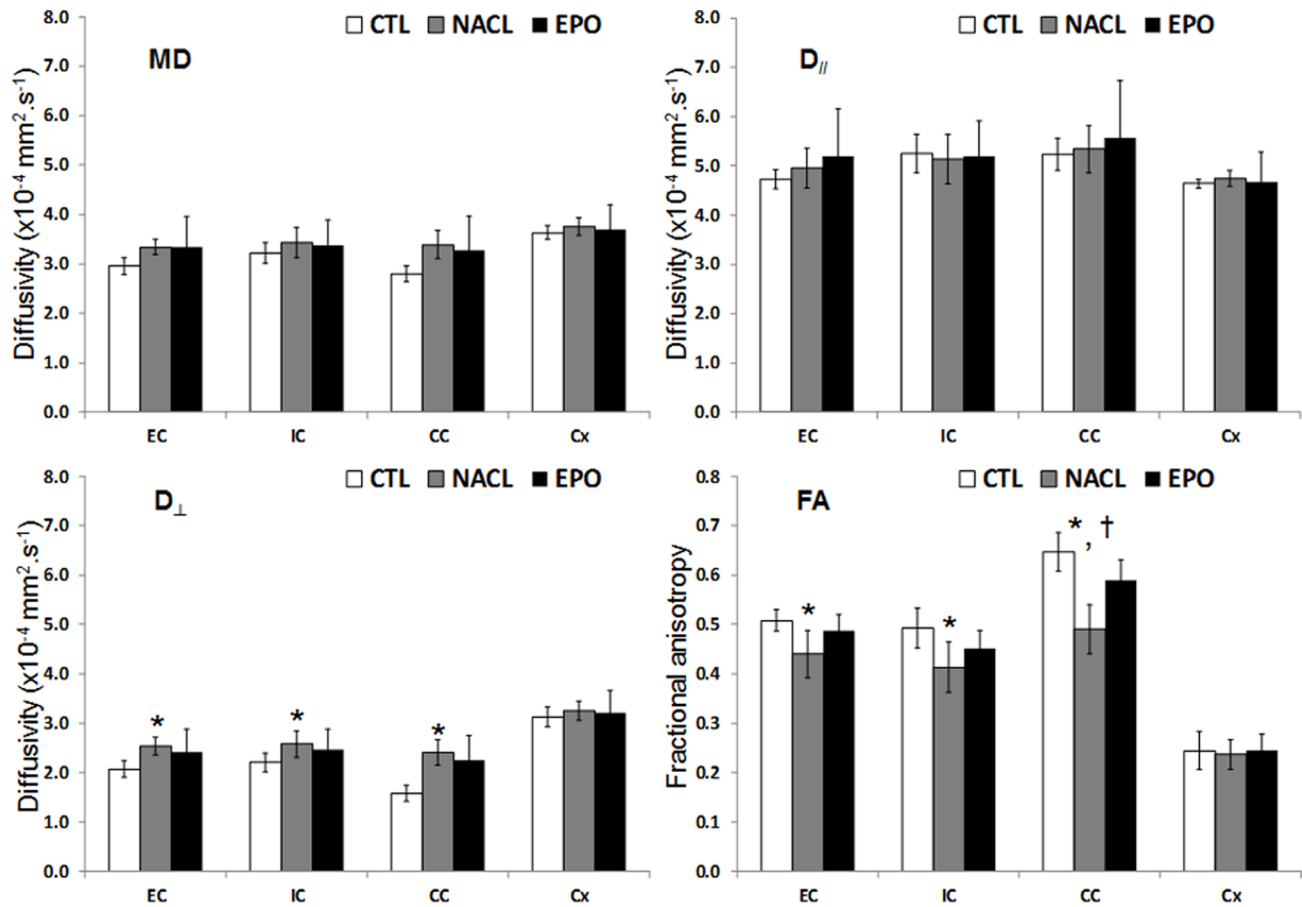


Figure 7. Microstructure assessment with DTI. Histogram of diffusivities (Mean: MD, axial: D_{\parallel} and radial: D_{\perp}) as well as fractional anisotropy (FA) values \pm SD measured in the in the external capsule (EC), internal capsule (IC), corpus callosum (CC) and cortex (Cx) of the EPO, NaCl and Control rats ($n=6$ rats for each group, NaCl, EPO and Control, mean values over the four different images planes corresponding to the one of the figure 6; *, †, ‡: $P<0.05$ NaCl vs. Control, EPO vs. Control and EPO vs. NaCl, respectively). doi:10.1371/journal.pone.0095643.g007

EPO-R [40]. In fetal sheep asphyxia model, expression of EPO-R was increased on astrocytes in brief asphyxia insult but required repeated asphyxia insults to be increased on neurons [41]. It also appears that EPO-R expression is different in the core of the injury compared to the penumbra and is mainly increased on apoptotic neurons [42]. Therefore, the moderate HI injury at P3 would lead to a weak increase of EPO receptors on neurons and exogenous EPO would be in excess compared to EPO-R with limited therapeutic effect as not bound to its target.

The presence of astrocytes might hamper the recovery of cortical tissue. High doses of EPO may have an adverse effect as it has been reported that high EPO dosage promotes the proliferation of astrocytes [43]. EPO exerts its neurotrophic role but in the same time activates astrocyte proliferation which accelerates oligodendrocytes maturation that should promote myelin repair [43].

Analyses of MBP staining showed no difference between the EPO and NaCl group neither in the corpus callosum nor in the internal capsule. Again dosage used might be implicated as high-dose of EPO (20 U/g) failed to restore myelination and function after neonatal HI in mice [30]. Nevertheless, in the same regions FA values were restored in the EPO group. The data obtained by *ex-vivo* DTI and SEP recordings showed that EPO has the potential to enhance white matter reorganization and gray matter functional recovery after injury. In the EPO group FA values

were restored to values comparable to control in white matter indicating microstructural recovery whereas the NaCl group showed lower FA than control indicating WM tract microstructure disruption. The discrepancy between MBP and microstructural assessment with FA is not surprising as not only the myelin influences FA in white matter but also axonal diameter or axonal compaction [44,45]. For instance, Favrais *et al.* observed reduced FA in several brain regions following inflammatory injury attributed to axonopathy [46]. Axonal evaluation using electronic microscopy would be necessary to address this question of an effect of EPO on axonal recovery or/and myelin compaction or axonal diameter. Importantly, SEP results indicate that EPO treatment induces functional recovery after HI injury that was not present in the animal that received NaCl only. Indeed, Iwai *et al.* [47] reported similar results in a neonatal rat model where administration of EPO was ineffective at decreasing infarct volume but significantly improved neurological function outcomes. These findings suggest that gross preservation of neural tissue is not a definite requirement for the recovery of neurological function and that EPO is beneficial for supporting neuronal plasticity and connectivity establishment. The restoration of neurological function is influenced by a variety of factors, such as the reorganization of surviving neuronal tissue, the restoration of myelin and oligodendrocytic architecture and gross anatomical recovery is less a prerequisite than improved connectivity. Chan *et al.* [48]

reported 10 weeks after HI injury induced at P9 on mice and without neuroprotective therapy an increased FA in several WM tracts attributed to WM reorganization despite a large loss of grey matter. EPO could stimulate this WM reorganization as depicted by the restoration of FA values in different WM tracts despite no gross anatomical recovery.

Conclusion

In this study we assessed the effects of long-term high dose of EPO following HI in the P3 pup rat with a multi-modal protocol. Such a protocol is very powerful to evaluate neuroprotective effects of EPO with a wide range of information including functional, macro- and micro-structural, metabolic and histologic assessment. In conclusion, long-term treatment with EPO in the P3 rat brain after HI injury showed functional recovery in the somatosensory cortex, partial white matter microarchitecture preservation and reduction of metabolic alterations despite

References

- Molnar Z, Rutherford M (2013) Brain maturation after preterm birth. *Science translational medicine* 5: 168ps162.
- Volpe JJ (2009) Brain injury in premature infants: a complex amalgam of destructive and developmental disturbances. *Lancet neurology* 8: 110–124.
- Clancy B, Darlington RB, Finlay BL (2001) Translating developmental time across mammalian species. *Neuroscience* 105: 7–17.
- Towfighi J, Mauger D, Vannucci RC, Vannucci SJ (1997) Influence of age on the cerebral lesions in an immature rat model of cerebral hypoxia-ischemia: a light microscopic study. *Developmental Brain Research* 100: 149–160.
- Sizonenko SV, Camm EJ, Dayer A, Kiss JZ (2008) Glial responses to neonatal hypoxic-ischemic injury in the rat cerebral cortex. *International journal of developmental neuroscience* 26: 37–45.
- Sizonenko SV, Kiss JZ, Inder T, Gluckman PD, Williams CE (2005) Distinctive neuropathologic alterations in the deep layers of the parietal cortex after moderate ischemic-hypoxic injury in the P3 immature rat brain. *Pediatric research* 57: 865–872.
- Sizonenko SV, Mayall Y, Sirimanne E, Gluckman PD, Inder T, et al. (2003) Selective Cortical Alteration after Hypoxic-Ischemic Injury in the Very Immature Rat Brain. *Pediatric research* 54: 263–269.
- Quairiaux C, Sizonenko SV, Megevand P, Michel CM, Kiss JZ (2010) Functional deficit and recovery of developing sensorimotor networks following neonatal hypoxic-ischemic injury in the rat. *Cerebral Cortex* 20: 2080–2091.
- Velly L, Pellegrini L, Guillet B, Bruder N, Pisano P (2010) Erythropoietin 2nd cerebral protection after acute injuries: a double-edged sword? *Pharmacology & therapeutics* 128: 445–459.
- Buemi M, Cavallaro E, Floccari F, Sturiale A, Aloisi C, et al. (2003) The pleiotropic effects of erythropoietin in the central nervous system. *Journal of neuropathology and experimental neurology* 62: 228–236.
- Kim MS, Seo YK, Park HJ, Lee KH, Choi EJ, et al. (2010) The neuroprotective effect of recombinant human erythropoietin via an antiapoptotic mechanism on hypoxic-ischemic brain injury in neonatal rats. *Korean journal of pediatrics* 53: 898–908.
- Sasaki R (2003) Pleiotropic functions of erythropoietin. *Intern Med* 42: 142–149.
- Bernaudin M, Bellail A, Marti HH, Yvon A, Vivien D, et al. (2000) Neurons and astrocytes express EPO mRNA: oxygen-sensing mechanisms that involve the redox-state of the brain. *Glia* 30: 271–278.
- Zhong Y, Yao H, Deng L, Cheng Y, Zhou X (2007) Promotion of neurite outgrowth and protective effect of erythropoietin on the retinal neurons of rats. *Graefes' archive for clinical and experimental ophthalmology* 245: 1859–1867.
- Aydin A, Genc K, Akhisaroglu M, Yorukoglu K, Gokmen N, et al. (2003) Erythropoietin exerts neuroprotective effect in neonatal rat model of hypoxic-ischemic brain injury. *Brain & development* 25: 494–498.
- Kumral A, Ozer E, Yilmaz O, Akhisaroglu M, Gokmen N, et al. (2003) Neuroprotective effect of erythropoietin on hypoxic-ischemic brain injury in neonatal rats. *Biology of the neonate* 83: 224–228.
- Kumral A, Uysal N, Tugyan K, Sonmez A, Yilmaz O, et al. (2004) Erythropoietin improves long-term spatial memory deficits and brain injury following neonatal hypoxia-ischemia in rats. *Behavioural brain research* 153: 77–86.
- Matsumita H, Johnston MV, Lange MS, Wilson MA (2003) Protective effect of erythropoietin in neonatal hypoxic ischemia in mice. *Neuroreport* 14: 1757–1761.
- van der Kooij MA, Groenendaal F, Kavelaars A, Heijnen CJ, van Bel F (2008) Neuroprotective properties and mechanisms of erythropoietin in vitro and in vivo experimental models for hypoxia/ischemia. *Brain research reviews* 59: 22–33.
- Juul S (2012) Neuroprotective role of erythropoietin in neonates. *Journal of Maternal-Fetal and Neonatal Medicine* 25 Suppl 4: 105–107.
- Shingo T, Sorokan ST, Shimazaki T, Weiss S (2001) Erythropoietin regulates the in vitro and in vivo production of neuronal progenitors by mammalian forebrain neural stem cells. *The journal of Neuroscience* 21: 9733–9743.
- Sizonenko SV, Bednarek N, Gressens P (2007) Growth factors and plasticity. *Seminars in fetal & neonatal medicine* 12: 241–249.
- Sola A, Wen TC, Hamrick SE, Ferriero DM (2005) Potential for protection and repair following injury to the developing brain: a role for erythropoietin? *Pediatric research* 57: 110R–117R.
- van de Looij Y, Chatagner A, Huppi PS, Gruetter R, Sizonenko SV (2011) Longitudinal MR assessment of hypoxic ischemic injury in the immature rat brain. *Magnetic Resonance in Medicine* 65: 305–312.
- Basser PJ, Pierpaoli C (1998) A simplified method to measure the diffusion tensor from seven MR images. *Magnetic Resonance in Medicine* 39: 928–934.
- van de Looij Y, Lodygensky GA, Dean J, Lazeyras F, Hagberg H, et al. (2012) High-field diffusion tensor imaging characterization of cerebral white matter injury in lipopolysaccharide-exposed fetal sheep. *Pediatric research* 72: 285–292.
- van de Looij Y, Mauconduit F, Beaumont M, Valable S, Farion R, et al. (2012) Diffusion tensor imaging of diffuse axonal injury in a rat brain trauma model. *NMR in biomedicine* 25: 93–103.
- Tkac I, Rao R, Georgieff MK, Gruetter R (2003) Developmental and regional changes in the neurochemical profile of the rat brain determined by in vivo ¹H NMR spectroscopy. *Magnetic Resonance in Medicine* 50: 24–32.
- Cerri G, Montagna M, Madaschi L, Merli D, Borroni P, et al. (2012) Erythropoietin effect on sensorimotor recovery after contusive spinal cord injury: an electrophysiological study in rats. *Neuroscience* 219: 290–301.
- Fan X, Heijnen CJ, van der KM, Groenendaal F, van Bel F (2011) Beneficial effect of erythropoietin on sensorimotor function and white matter after hypoxia-ischemia in neonatal mice. *Pediatric research* 69: 56–61.
- McPherson RJ, Juul SE (2008) Recent trends in erythropoietin-mediated neuroprotection. *International Journal of Developmental Neuroscience* 26: 103–111.
- Traudt CM, Juul SE (2013) Erythropoietin as a neuroprotectant for neonatal brain injury: animal models. *Methods in Molecular Biology* 982: 113–126.
- Mlynarik V, Gambarota G, Frenkel H, Gruetter R (2006) Localized short-echo-time proton MR spectroscopy with full signal-intensity acquisition. *Magnetic Resonance in Medicine* 56: 965–970.
- Provencher SW (1993) Estimation of metabolite concentrations from localized in vivo proton NMR spectra. *Magnetic Resonance in Medicine* 30: 672–679.
- Rivière D, Régis J, Cointepas Y, Papadopoulos-Orfanos D, Cachia A, et al. (2003) A freely available Anatomist/BrainVISA package for structural morphometry of the cortical sulci. *NeuroImage* 19: 934.
- Troncoso E, Muller D, Czellar S, Zoltan Kiss J (2000) Epicranial sensory evoked potential recordings for repeated assessment of cortical functions in mice. *Journal of neuroscience methods* 97: 51–58.
- van de Looij Y, Kunz N, Huppi P, Gruetter R, Sizonenko S (2011) Diffusion tensor echo planar imaging using surface coil transceiver with a semiadiabatic RF pulse sequence at 14.1T. *Magnetic Resonance in Medicine* 65: 732–737.
- Sun SW, Neil JJ, Song SK (2003) Relative indices of water diffusion anisotropy are equivalent in live and formalin-fixed mouse brains. *Magnetic Resonance in Medicine* 50: 743–748.
- Iwai M, Cao G, Yin W, Stetler RA, Liu J, et al. (2007) Erythropoietin promotes neuronal replacement through revascularization and neurogenesis after neonatal hypoxia/ischemia in rats. *Stroke* 38: 2795–2803.

Acknowledgments

This work was supported by the Centre d'Imagerie Biomédicale (CIBM) of the Université de Genève (UNIGE), Université de Lausanne (UNIL), Hôpitaux Universitaires de Genève (HUG), Centre Hospitalier Universitaire Vaudois Lausanne (CHUV), Ecole Polytechnique Fédérale de Lausanne (EPFL) and the Lenards and Jeantet Foundations.

Author Contributions

Conceived and designed the experiments: YVDL AC CQ RG PSH SVS. Performed the experiments: YVDL AC CQ. Analyzed the data: YVDL AC CQ. Contributed reagents/materials/analysis tools: YVDL AC CQ. Wrote the paper: YVDL AC CQ PSH SVS.

40. Chin K, Yu X, Beleslin-Cokic B, Liu C, Shen K, et al. (2000) Production and processing of erythropoietin receptor transcripts in brain. *Brain research Molecular brain research* 81: 29–42.
41. Castillo-Melendez M, Yan E, Walker DW (2005) Expression of erythropoietin and its receptor in the brain of late-gestation fetal sheep, and responses to asphyxia caused by umbilical cord occlusion. *Developmental neuroscience* 27: 220–227.
42. Wen TC, Rogido M, Genetta T, Sola A (2004) Permanent focal cerebral ischemia activates erythropoietin receptor in the neonatal rat brain. *Neuroscience letters* 355: 165–168.
43. Sugawa M, Sakurai Y, Ishikawa-Ieda Y, Suzuki H, Asou H (2002) Effects of erythropoietin on glial cell development; oligodendrocyte maturation and astrocyte proliferation. *Neuroscience research* 44: 391–403.
44. Barazany D, Bassar PJ, Assaf Y (2009) In vivo measurement of axon diameter distribution in the corpus callosum of rat brain. *Brain* 132: 1210–1220.
45. Kunz N, Sizonenko SV, Huppi PS, Gruetter R, van de Looij Y (2013) Investigation of field and diffusion time dependence of the diffusion-weighted signal at ultrahigh magnetic fields. *NMR in biomedicine* 26: 1251–1257.
46. Favrais G, van de Looij Y, Fleiss B, Ramanantsoa N, Bonnin P, et al. (2011) Systemic inflammation disrupts the developmental program of white matter. *Annals of neurology* 70: 550–565.
47. Iwai M, Stetler RA, Xing J, Hu X, Gao Y, et al. (2010) Enhanced oligodendrogenesis and recovery of neurological function by erythropoietin after neonatal hypoxic/ischemic brain injury. *Stroke* 41: 1032–1037.
48. Chan KC, Khong PL, Lau HF, Cheung PT, Wu EX (2009) Late measures of microstructural alterations in severe neonatal hypoxic-ischemic encephalopathy by MR diffusion tensor imaging. *International journal of developmental neuroscience* 27: 607–615.